SEGMENTATION OF MACULAR LAYERS IN OCT DATA OF TOPOLOGICALLY DISRUPTED MACULA

Athira S C[1], Reena M Roy[2]
[1]P G Scholar, L.B.S Institute of Technology for women Poojappura Trivandrum,
[2]Assistant Professor, L.B.S Institute of Technology for women Poojappura Trivandrum

Abstract

Optical coherence tomography (OCT) is an established medical imaging technique that uses light to capture micrometer–resolution, images. The images from OCT can be used in the investigation of various Macular Disorders. The thicknesses of the macular layers are affected during multiple eye disorders. The accurate quantification of the macular layers and lesions provides clinically relevant information about macula. But the extraction and study of the OCT images manually is the time consuming and prone to human errors. The currently existing approaches focus on extracting data about a specific lesion in the diseased macula or on segmenting the macular layers in the healthy macula, thereby avoiding much valuable clinical information. The new automatic method is an approach to jointly segment macular layers and lesion in eyes with topology disrupting macular disorders. This method is capable of handling local intensity variation and the presence or absence of pathological structure in the macula. Thus it provides a flexible and accurate method to study the OCT images.

Index Terms: Optical Coherence Tomography, Macular Edema, Age related macular degeneration, Ganglion cell complex, Outer nuclear layer, Central serous retinopathy.

I. INTRODUCTION

Optical coherence tomography (OCT) is a noninvasive, and latest eye examination technique that can be used to acquire in-vivo images of macular structures. Its high resolution enables the investigation of the macular tissue layers and pathological changes [1]. In various eye disorders, the thickness of one or more macular layers is affected. For example, ganglion cell complex (GCC) gets thinner in patients with age-related macular degeneration (AMD). Furthermore, changes in the properties of a tissue that composes a layer occur [2]. For example, in patients with glaucoma, the OCT signal and OCT derived attenuation coefficient values of the RNFL were shown to be reduced when compared to healthy subjects, whereas in patients with central serous retinopathy (CSR), changes in reflectivity of the outer nuclear layer (ONL) were encountered. Finally, certain pathologies may give rise to additional structures that are not present in the macula of healthy subjects. In dry AMD, small deposits of extracellular tissue, called drusen, form within the retina. In CSR, the build-up of fluids in the macula space creates a fluid pocket that disrupts the outer macular layers. In diabetic macular edema (DME), cysts may form inside inner and outer macula layers. Accurate quantification of macula structures, both layers and lesions, provides clinically relevant information about the macula. Extraction of these imaging biomarkers has become an important task as it enables valuable input for diagnostics, prognostics, and monitoring of macular disorders [1]. When done manually, this is a potentially subjective and time-consuming job and large data volumes. Hence, an objective and automated tool that extracts clinically useful information, such as the thickness of layers and the presence and extent of

emerging pathologies, is needed. This need for segmentation of macular layers and lesions has been recognized before [1]. However, most existing approaches focus either on extracting information about a specific lesion in the diseased macula or on segmenting the macular layers in healthy macula and macular disorders such as macular edema (ME), AMD, CSR etc. By segmenting only macula lesions without macular layer segmentation, other potentially valuable clinical information about the macula is ignored. Automatic segmentation of the both macular layers and lesions that may exist in pathological macula, such as sub retinal fluid, drusen and cysts, remains a challenging task as the presence of lesions can cause large disruptions of the macula. First, the topology and morphology of the macula may be affected. Second, the lesions vary largely in size, shape and location. Third, the OCT intensity of one or more layers may vary considerably within a scan. A few approaches have been presented to segment both the macular layers and lesions but only three of these approaches have the accuracy of both layer and lesion segmentation evaluated.

Fig.1: OCT

II. METHODOLOGY

The segmentation framework performs the joint segmentation of interfaces between macular layers and lesions. It operates on attenuation coefficients, which are derived from in-vivo human macular OCT images. The framework consists of several processing steps including conversion to attenuation coefficients, feature detection, noise suppression as well as the actual joint layer and lesion segmentation method. First, briefly introduce the conversion to attenuation coefficients and the LCLS framework. Then, generalizations to the framework to deal with segmentation challenges present in the eyes of CSR and AMD patients such as the local variation in estimated attenuation coefficients within layers and the presence of space-variant lesions.

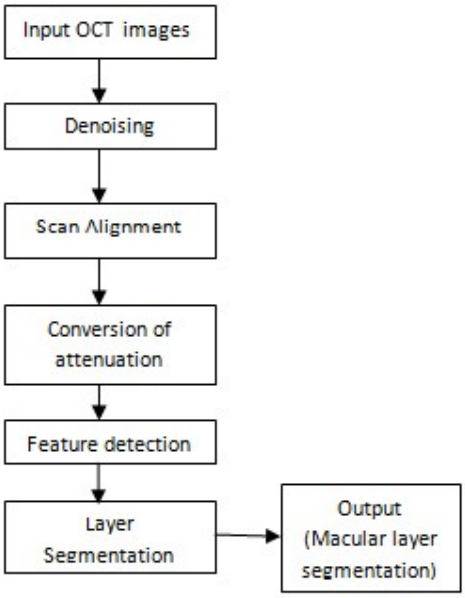

Fig.2: Block Diagram

A. *Attenuation coefficient*

The intensities of the raw OCT data were compensated for noise and depth-dependent decay after which the OCT data was transformed into attenuation coefficients. The attenuation coefficient is an optical property of a tissue and as such illumination invariant. Therefore, various arte facts that are common in OCT images, such as intensity fluctuation within layers, are largely reduced. In short, the calculation of the attenuation coefficients is performed based on the ratio of intensity at a certain depth and summation of intensities beyond that depth. The intensity value at a certain depth represents the back-scattered light at that depth, whereas the summation represents the amount of light that is back-scattered at depths beyond the current one. The ratio of the two can be understood as the fraction of the incident light that is back-scattered.

B. *Loosely coupled level sets (LCLS)*

The LCLS framework employs a probabilistic approach, which incorporates image data and prior knowledge of the macula to segment the interfaces between macular layers. Every Interface Ci is represented by its

own level set function ϕi, which is propagated according to the equation 1

$$\frac{d\phi i}{dt} = -\Delta t((Pr(li|\mu)-0.5)+\alpha ki+\beta\zeta i)|\Delta\Phi i| \quad (1)$$

Where Pr(li|μ) is the probability of a pixel belonging to layer li given the attenuation coefficient μ of that pixel, and ki and ζi the geometric regularization terms. The weights of the terms are denoted by α and ß, while Δt is the time step. The probabilistic term expresses the posterior probability of pixels along an interface belonging to the retinal layer above the interface (li) as:

$$Pr(li|\mu)=\frac{Pr(\mu|li)Pr(li)}{\sum_{j\in\{i,i+1\}} Pr(\mu|lj)Pr(lj)} \quad (2)$$

Where Pr(li|μ) is the likelihood based on the available image data inside the set Ωi containing all pixels assigned to layer li, and Pr(li) is the prior for layer li. The prior probability combines prior knowledge on the attenuation coefficient values and on the order of the layers and their thickness. Finally, the probability density function Pr(μ|li) can be approximated by the normalized histogram Pr(μ|Ωi) of all pixels assigned to layer li. In some cases, the layers are no longer homogeneous but show large attenuation coefficient variations, which affect both the likelihood estimation as well as the use of prior knowledge. Furthermore, the presence of lesions impacts both the topology and morphology of the macula.

C. *Lesion segmentation*

In CSR, fluid accumulates above the RPE and creates a sub retinal fluid pocket. In our framework, this fluid is modeled as an additional layer present within another retinal layer surrounded by the IS ellipsoids and the posterior RPE boundary. Hence, two auxiliary interfaces are introduced. These auxiliary interfaces are propagated according to equation 1 by utilizing the difference in the estimated attenuation coefficient values of the surrounding layers and prior knowledge. Prior knowledge about the order of layers was enforced such that the fluid is contained between the IS ellipsoids and the posterior RPE boundary. However, no prior knowledge on the thickness of the fluid pocket was imposed. As mentioned, in areas and scans without lesions, the additional layer may shrink to a near zero thickness. In practice, the layer had a thickness varying between 0 - 3.9μm, i.e. less than one pixel. Therefore, a thickness of less than 3.9μm was interpreted to indicate that no lesion was present at that location. In AMD, disruption of the RPE occurs and extracellular material starts to accumulate resulting in the formation of drusen. As a result of this disruption, Bruch's membrane becomes separated from the posterior RPE boundary. However, the membrane is only visible below the drusen, whereas in areas and eyes without drusen it remains adjacent to the posterior RPE boundary and cannot be discerned. Therefore, drusen can be considered as a layer between the posterior RPE boundary and Bruch's membrane. As one of the boundaries of drusen coincides with an interface between retinal layers, only one auxiliary interface is introduced which corresponds to the Bruch's membrane. The segmentation of Bruch's membrane is frequently obtained by taking a convex envelope of the posterior RPE boundary. All elevation of the posterior RPE boundary higher that 20μm and larger than 25μm in diameter.

D. *Initialization*

Propagation of the level set functions is done by simultaneously solving the set of partial differential equations that drive the current segmentation of the retinal interfaces to its minimum energy state. The initialization stage of the segmentation framework, that is based on a minimum cost path search and that is applied to individual B-scans, was adapted to accommodate the possible presence of lesions. The cost function for the posterior RPE boundary was modified and instead of initializing ellipsoid boundary was initialized. Two additional nodes with zero cost, that connect each pixel in the first and the last A-scans were added, to make the initialization process fully automatic. The RPE is primarily a horizontal layer. However, in eyes affected by dry AMD, drusen appear as vertical elevations of the posterior RPE boundary and the RPE is no longer approximately horizontal. Our previously used cost function for the posterior RPE boundary was based on the derivative in the z-direction (as the RPE was horizontal). Due to vertical changes in the RPE, our new approach also included the derivative in the x-direction in

the cost function (fc), which was defined as follows: Fc=(1-(gz*I)/(max(gz*I)))+(1 - (abs(gx*I))/max(abs(gx*I))) (3) Where I stand for a B-scan, gz and gx are Gaussian derivatives in the z- and x-direction, respectively. For other interfaces (the vitreous-RNFL and IS ellipsoid boundary),
only the derivative in the z-direction is considered and the cost function is defined as follows:
Fc=1-(gz*I)/(max(gz*I)).The initialization was performed in a sequential manner, by first initializing the posterior RPE boundary. Then, the vitreous-RNFL interface was initialized by limiting the search region to the area above the posterior RPE boundary. Finally, the IS ellipsoid boundary was found by limiting the search area to the region bounded by the vitreous-RNFL interface and the posterior RPE boundary.

III. RESULT AND DISCUSSION

The results represents the Manual and automatic detection of macular disorders. The Automatic detection means the automatically layer detected image can be obtained, from the layer segmented images we can find out the abnormalities of the macula. From this abnormality we can obtain macular disorders automatically. This also helps ophthalmologist to treat the patient with high accuracy rate.

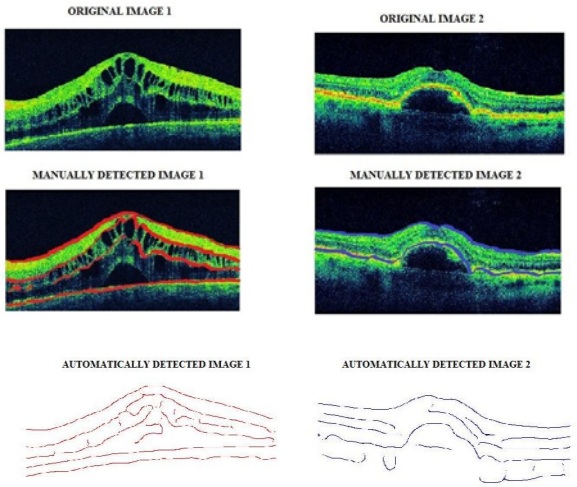

Fig.3: Automatic and Manual layer Detection of Macular disorder.

IV. CONCLUSION AND FUTURESCOPE

The macular disorders are one of the leading causes of blindness among majority. There is no accurate and automatic method for detection of macular disorders. This paper proposed automatic layer segmentation for macular disorders like macular edema. The segmented OCT images can be utilized to detect various Macular diseases at earlier stages. Specific algorithms or trained classifiers can be developed to categorize the diseases. Further optimization of the algorithm can speed up the evaluations thereby diagnosing the diseases in mean time. A more effective and extensive evaluations of eyes with or without the lesions in such a way that it can help in diagnosing all sorts of Macular disorders.

REFERENCES

[1] Novosel, Jelena, et al. "Joint Segmentation of Retinal Layers and Focal Lesions in 3-D OCT Data of Topologically Disrupted Retinas." *IEEE Transactions on Medical Imaging* 36.6 (2017): 1276-1286.J. U. Duncombe, "Infrared navigation—Part I: An assessment of feasibility," IEEE Trans. Electron Devices, vol. ED-11, pp. 34-39, Jan. 1959.

[2] Shi, Fei, et al. "Automated 3-D retinal layer segmentation of macular optical coherence tomography images with serous pigment epithelial detachments." *IEEE transactions on medical imaging* 34.2 (2015): 441-452.

[3] Hassan, Taimur, et al. "Review of OCT and fundus images for detection of Macular Edema." *Imaging Systems and Techniques (IST), 2015 IEEE International Conference on*. IEEE, 2015.

[4] Hassan, Bilal, et al. "Structure tensor based automated detection of macular edema and central serous retinopathy using optical coherence tomography images." *JOSA A* 33.4 (2016): 455-463.

[5] Novosel, Jelena, et al. "Joint Segmentation of Retinal Layers and Focal Lesions in 3-D OCT Data of Topologically Disrupted Retinas." *IEEE Transactions on Medical Imaging* 36.6 (2017): 1276-1286.

[6] Strøm, Charlotte, et al. "Diabetic macular edema assessed with optical coherence tomography and stereo fundus photography." *Investigative ophthalmology & visual science*43.1 (2002): 241-245.

[7] Gilbert, Clare E., et al. "Poverty and blindness in Pakistan: results from the

Pakistan national blindness and visual impairment survey." *Bmj* 336.7634 (2008): 29-32.

[8] Sinthanayothin, Chanjira, et al. "Automated detection of diabetic retinopathy on digital fundus images." *Diabetic medicine* 19.2 (2002): 105-112.

[9] Deepak, K. Sai, and Jayanthi Sivaswamy. "Automatic assessment of macular edema from color retinal images." *IEEE Transactions on medical imaging* 31.3 (2012): 766-776.

[10] Faust, Oliver, et al. "Algorithms for the automated detection of diabetic retinopathy using digital fundus images: a review." *Journal of medical systems* 36.1 (2012): 145-157.

[11] Ciulla, Thomas A., Armando G. Amador, and Bernard Zinman. "Diabetic retinopathy and diabetic macular edema." *Diabetes care* 26.9 (2003): 2653-2664.

[12] Kunwar, Aditya, Shrey Magotra, and M. Partha Sarathi. "Detection of high-risk macular edema using texture features and classification using SVM classifier." *Advances in Computing, Communications and Informatics (ICACCI), 2015 International Conference on*. IEEE, 2015.

[13] Massich, Joan, et al. "Classifying DME vs normal SD-OCT volumes: A review." *Pattern Recognition (ICPR), 2016 23rd International Conference on*. IEEE, 2016.